

Dodecanuclear and octanuclear manganese rods

Euan K. Brechin,^{*a} Monica Soler,^b George Christou,^b Madeleine Helliwell,^a Simon J. Teat^c and Wolfgang Wernsdorfer^d^a Department of Chemistry, The University of Manchester, Oxford Road, Manchester, UK M13 9PL.

E-mail: euan.k.brechin@man.ac.uk; Tel: 0161-275-7857

^b Department of Chemistry, University of Florida, Gainesville, Florida 32611-7200, USA^c CLRC Daresbury Laboratory, Daresbury, Warrington, Cheshire, UK WA4 4AD^d Laboratoire Louis Néel-CNRS, 38042 Grenoble, Cedex 9, France

Received (in Cambridge, UK) 21st February 2003, Accepted 3rd April 2003

First published as an Advance Article on the web 23rd April 2003

The reaction of the neutral triangle $[\text{Mn}_3\text{O}(\text{O}_2\text{CR})_6(\text{L})_3]$ with 1,1,1-tris(hydroxymethyl)ethane (H_3thme) affords novel dodecanuclear and octanuclear manganese complexes with unusual ladder-like cores built from edge-sharing triangles.

The synthesis of polynuclear transition metal clusters has recently been driven by the discovery that molecules with large numbers of unpaired electrons can function as nanoscale magnets.¹ The first single-molecule magnet (SMM) $[\text{Mn}_{12}\text{O}_{12}(\text{OAc})_{16}(\text{H}_2\text{O})_4]$ was discovered in 1993 and since then the vast majority of SMMs reported have contained either manganese or iron.² Each of these SMMs has been synthesised using an appropriate metal and coordinatively flexible organic ligands such as carboxylates, β -diketonates and alkoxides. The tripodal ligand 1,1,1-tris(hydroxymethyl)ethane (H_3thme) has been used extensively in the synthesis of oxovanadium and oxomolybdenum clusters³ but has been sparingly used with other metals.⁴ Following our initially encouraging results using this ligand with manganese and iron,^{5,6} we herein report the synthesis, structure and initial magnetic properties of new dodecanuclear and octanuclear manganese rods based on a series of edge-sharing Mn_3 units.

The reaction of the triangular Mn^{2+} , Mn^{3+} complex $[\text{Mn}_3\text{O}(\text{PhCOO})_6(\text{py})_2(\text{H}_2\text{O})]$ with 1 equivalent of H_3thme in MeCN gives the mixed-valent complex $[\text{Mn}_{12}\text{O}_4(\text{OH})_2(\text{PhCOO})_{12}(\text{thme})_4(\text{py})_2]$ **1**, in moderate yield upon diffusion of Et_2O , after 3 days. Complex **1** (Fig. 1) crystallises in the monoclinic space group $P2_1/c$. The core of **1** consists of a

$[\text{Mn}^{\text{III}}_{10}\text{Mn}^{\text{II}}_2\text{O}_4(\text{OH})_2]^{24+}$ ladder-like unit where Mn1 and Mn12 are, respectively, above and below the plane of the central ten Mn ions. The $[\text{Mn}^{\text{III}}_{10}\text{Mn}^{\text{II}}_2\text{O}_4(\text{OH})_2]^{24+}$ core is trapped-valence, with Mn3 and Mn10 being the Mn^{2+} ions, and can be described as consisting of ten edge-sharing $[\text{Mn}_3\text{O}]$ triangles or five edge-sharing $[\text{Mn}_4\text{O}_2]$ butterfly units. All twelve Mn ions are in distorted octahedral geometries with the ten Mn^{3+} ions displaying the expected Jahn-Teller elongations. The four thme^{3-} ligands are fully deprotonated, sitting directly above and below the $[\text{Mn}^{\text{III}}_{10}\text{Mn}^{\text{II}}_2\text{O}_4(\text{OH})_2]^{24+}$ plane, and are of two types: two use two of their arms in a μ_2 -fashion with the third arm acting as a μ_3 -bridge; the reverse situation applies for the other two thme^{3-} ligands which have two μ_3 -arms and one μ_2 -arm. The PhCO_2^- ligands bridge in their usual μ_2 -manner with the remaining coordination sites occupied by two pyridines. The four O^{2-} (O1, O18, O22, O34) and two OH^- ions (O19, O23) ligands are μ_3 - and μ_2 -bridging respectively.

Replacement of PhCO_2^- with $(\text{CH}_3)_3\text{CCO}_2^-$ (piv^-) in the triangular starting material produces the related octanuclear complex $[\text{Mn}_8\text{O}_4(\text{piv})_{10}(\text{thme})_2(\text{py})_2]$ **2**. Complex **2** (Fig. 1) crystallises in the monoclinic space group $P2_1/c$ in good yield after 2 days. The core of **2** consists of a $[\text{Mn}^{\text{III}}_8\text{O}_4]^{16+}$ ladder-like unit with Mn1 and Mn8 above and below the plane of the central six Mn ions (Mn2, Mn3 and Mn4). In this case the core can be described as six edge-sharing triangles or three edge-sharing butterfly units. All eight Mn^{3+} ions are in distorted octahedral geometries and display the Jahn-Teller elongations expected for high spin Mn^{3+} . The two thme^{3-} ligands are deprotonated and sit above and below the plane of the central six Mn^{3+} ions each using two arms in a μ_2 -fashion and one arm in a μ_3 -fashion. The piv^- ligands bridge in their usual μ_2 -fashion with the two pyridines again providing the capping for the terminal sites on Mn1 and Mn1A. All oxidation states were assigned using charge balance considerations, bond lengths and bond valence sum calculations. The structure of **2** is clearly related to **1** and can be thought of as **1** with a “ $[\text{Mn}_4(\text{O}(\text{H})_2(\text{O}_2\text{CR})_2(\text{thme})_2)]$ ” fragment missing and containing only Mn^{3+} ions. These rod or ladder-like structures represent a new topology in Mn cluster chemistry.

Solid-state dc magnetization measurements were performed on **1** in the range 5–300 K in a field of 5.0 kG. The $\chi_{\text{M}}T$ value of approximately $30 \text{ cm}^3 \text{ K mol}^{-1}$ at 300 K remains constant as the temperature is decreased until ca. 150 K when it begins to decrease to a value of ca. $25 \text{ cm}^3 \text{ K mol}^{-1}$ at 8K, suggesting that the molecule has a high spin ground state. In order to determine the ground state spin, magnetization data were collected in the ranges 1.8–10 K and 0.10–4.0 T. The data were fit giving $S = 7$, $g = 1.98$ and $D = -0.13 \text{ K}$. When fields up to 7 T were employed the best fit gave $S = 10$, $g = 1.78$ and $D = -0.30 \text{ K}$, but this was of poorer quality than the low field data. This behaviour is characteristic of low-lying excited states with S values greater than the ground state of $S = 7$. Low-lying excited states are a common problem when Mn^{2+} ions are present since they exhibit weak exchange coupling. The use of only low-field data in the fits can avoid this problem and provide more reliable results.

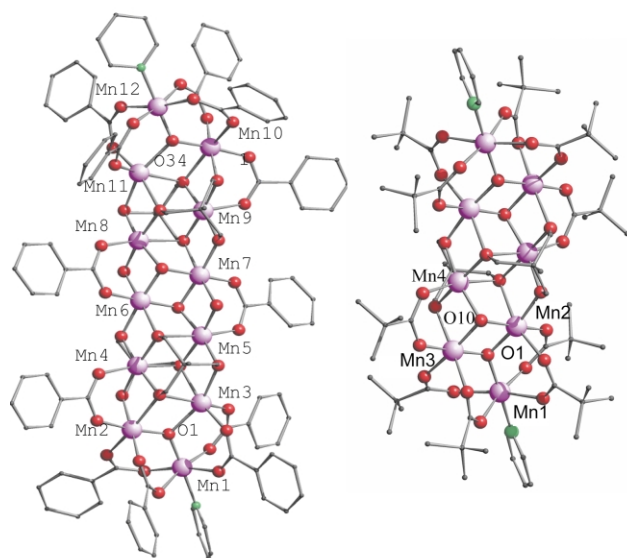


Fig. 1 The structure of complex **1** (left). Selected inter-atomic distances (Å); $\text{Mn}^{3+}\text{-O}$, 1.795(5)–2.335(5); $\text{Mn}^{2+}\text{-O}$ 2.087(6)–2.334(5). The structure of complex **2** (right). Selected inter-atomic distances (Å); $\text{Mn}^{3+}\text{-O}$, 1.829(5)–2.309(5).

DOI: 10.1039/b302057f

For complex **2**, the $\chi_M T$ value at 300 K of approximately $24 \text{ cm}^3 \text{ K mol}^{-1}$ drops slowly as the temperature is decreased until ca. 20 K where it then increases to a value of ca. $18 \text{ cm}^3 \text{ K mol}^{-1}$ at 8 K. Again this suggests that the molecule has a high spin ground state. Magnetization data (Fig. 2) collected in the ranges 1.8–10 K and 0.10–4.0 T gave a best fit of $S = 6$, $g = 1.81$ and $D = -0.36 \text{ K}$. The large spin ground states for both complexes presumably arise from the triangular $[\text{Mn}_3]$ building blocks in each cluster and thus the presence of a number of competing exchange interactions.

Ac magnetization measurements were performed on **1** and **2** in the 1.8–10 K range in a 3.5 G ac field oscillating at 50–1000 Hz. For both complexes frequency dependent ac signals are seen below approximately 3 K but no peaks are observed.

Quantum tunnelling of magnetization (QTM) studies were performed on **1** by magnetization measurements on single crystals using an array of micro-SQUIDS.⁷ Relaxation data were determined from dc relaxation decay measurements: first a field of 1.4 T was applied to the sample at 5 K to saturate the magnetization in one direction, and the temperature lowered to a chosen value between 1.5 and 0.04 K. The field was then swept to 0 T at 0.14 T s^{-1} and the magnetization in zero field measured as a function of time. From these data, relaxation times could be extracted which allows the construction of an Arrhenius plot which contains two distinct features. Above ca. 0.3 K the relaxation rate is temperature-dependent with $\tau_0 = 1.6 \times 10^{-7} \text{ s}$ and $U_{\text{eff}} = 18.3 \text{ K}$. Below ca. 0.3 K however, the relaxation rate is temperature-independent with a relaxation rate of $3 \times 10^7 \text{ s}$ indicative of QTM between the ground states. Hysteresis loops (Fig. 2) obtained at temperatures below 1.2 K, with sweep rates of 0.07 T s^{-1} , and with the field applied in the

direction of the easy axis, show steps at regular intervals of ca. 0.24 T ($D/g = 0.16 \text{ K}$) indicative of QTM. Single crystal studies of **2** are currently under way and will be reported at a later date.

In summary compounds **1** and **2** represent new structural types in manganese carboxylate chemistry and **1** is an important new addition to the small family of SMMs. It also suggests that the use of triangular building blocks is an excellent way to make large metal clusters with non-zero spin ground states.

This work was supported by Lloyd's of London Tercentenary Foundation and the National Science Foundation.

Notes and references

† Complex **1** analysed satisfactorily (C, H, N) as $1 \cdot \text{MeCN} \cdot \text{Et}_2\text{O}$. Complex **2** analysed satisfactorily (C, H, N) as $2 \cdot \text{MeCN} \cdot \text{Et}_2\text{O}$. Crystals were kept in contact with mother liquor to avoid solvent loss and were crystallographically identified as $1 \cdot 2.25\text{Et}_2\text{O}$ and $2 \cdot 4\text{MeCN} \cdot 3\text{H}_2\text{O}$.

‡ Crystal data for **1**: $\text{C}_{114}\text{H}_{108}\text{Mn}_{12}\text{N}_2\text{O}_{42} \cdot 2.25\text{Et}_2\text{O}$, monoclinic, $P2_1/c$, $a = 18.4232(10)$, $b = 28.2986(15)$, $c = 26.5871(14) \text{ \AA}$, $\alpha = 90^\circ$, $\beta = 90.085(2)^\circ$, $\gamma = 90^\circ$, $V = 13861.2(13) \text{ \AA}^3$, $M = 3004.07$, $Z = 4$, $T = 150(2) \text{ K}$, $\mu = 1.132 \text{ mm}^{-1}$, Synchrotron radiation (CLRC Daresbury Laboratory, Station 9.8, $\lambda = 0.6867 \text{ \AA}$), 61081 reflections collected, 19860 unique, ($R_{\text{int}} = 0.0492$) $2\theta_{\text{max}} = 44.83^\circ$, $R1 = 0.0732$ [13320 data with $I > 2\sigma(F)$], $wR2 = 0.2086$ for 1815 parameters. Crystal data for **2**: $\text{C}_{70}\text{H}_{118}\text{Mn}_8\text{N}_2\text{O}_{30} \cdot 4\text{MeCN} \cdot 3\text{H}_2\text{O}$, monoclinic, $P2_1/c$, $a = 17.332(2)$, $b = 12.552(2)$, $c = 25.289(3) \text{ \AA}$, $\alpha = 90^\circ$, $\beta = 108.864(7)^\circ$, $\gamma = 90^\circ$, $V = 5203.1(12) \text{ \AA}^3$, $M = 2122.42$, $Z = 2$, $T = 150(2) \text{ K}$, $\mu = 1.012 \text{ mm}^{-1}$, Synchrotron radiation (CLRC Daresbury Laboratory, Station 9.8, $\lambda = 0.6845 \text{ \AA}$), 7735 reflections collected, 5119 unique, ($R_{\text{int}} = 0.0359$) $2\theta_{\text{max}} = 40^\circ$, $R1 = 0.0572$ [3639 data with $I > 2\sigma(F)$], $wR2 = 0.1574$ for 533 parameters. Data collection, structure solution and refinement used programs SMART,⁹ SAINT¹⁰ and SHELXL.¹¹ CCDC 204631 and 204632. See <http://www.rsc.org/suppdata/cc/b3/b302057f/> for crystallographic data in .cif or other electronic format.

- R. Sessoli, H.-L. Tsai, A. R. Schake, S. Wang, J. B. Vincent, K. Folting, D. Gatteschi, G. Christou and D. N. Hendrickson, *J. Am. Chem. Soc.*, 1993, **115**, 1804.
- D. N. Hendrickson, G. Christou, H. Ishimoto, J. Yoo, E. K. Brechin, A. Yamaguchi, E. M. Rumberger, S. M. J. Aubin, Z. Sun and G. Aromi, *Polyhedron*, 2001, **20**, 1479; E. K. Brechin, C. Boskovic, W. Wernsdorfer, J. Yoo, A. Yamaguchi, E. C. Sanudo, T. R. Concolino, A. L. Rheingold, H. Ishimoto, D. N. Hendrickson and G. Christou, *J. Am. Chem. Soc.*, 2002, **124**, 9710; C. Boskovic, E. K. Brechin, W. E. Streib, K. Folting, J. C. Bollinger, D. N. Hendrickson and G. Christou, *J. Am. Chem. Soc.*, 2002, **124**, 3725; J. Yoo, E. K. Brechin, A. Yamaguchi, M. Nakano, J. C. Huffman, A. L. Maniero, L.-C. Brunel, K. Awaga, H. Ishimoto, G. Christou and D. N. Hendrickson, *Inorg. Chem.*, 2000, **39**, 3615; C. Sangregorio, T. Ohm, C. Paulsen, R. Sessoli and D. Gatteschi, *Phys. Rev. Lett.*, 1997, **78**, 4645; A. L. Barra, A. Caneschi, A. Cornia, F. F. De Biani, D. Gatteschi, C. Sangregorio, R. Sessoli and L. Sorace, *J. Am. Chem. Soc.*, 1999, **121**, 5302; C. Benelli, J. Cano, Y. Journaux, R. Sessoli, G. A. Solan and R. E. P. Winpenny, *Inorg. Chem.*, 2001, **40**, 188.
- M. I. Khan and J. Zubieta, *Prog. Inorg. Chem.*, 1995, **43**, 1.
- R. C. Finn and J. Zubieta, *J. Cluster Sci.*, 2000, **11**, 461; M. Cavaluzzo, Q. Chen and J. Zubieta, *Chem. Commun.*, 1993, 131; K. Hegetschweiler, H. Schmalke, H. M. Streit and W. Schneider, *Inorg. Chem.*, 1990, **29**, 3625; A. Cornia, D. Gatteschi, K. Hegetschweiler, L. Hausher-Primo and V. Gramlich, *Inorg. Chem.*, 1996, **35**, 4414.
- E. K. Brechin, M. Soler, J. Davidson, D. N. Hendrickson, S. Parsons and G. Christou, *Chem. Commun.*, 2002, 2252.
- L. F. Jones, A. Batsanov, E. K. Brechin, D. Collison, M. Helliwell, T. Mallah, E. J. L. McInnes and S. Piligkos, *Angew. Chem., Int. Ed.*, 2002, **22**, 4318.
- W. Wernsdorfer, *Adv. Chem. Phys.*, 2001, **118**, 99.
- R. J. Cernik, W. Clegg, C. R. A. Catlow, G. Bushnell-Wye, J. V. Flaherty, G. N. Greaves, I. Burrows, D. J. Taylor, S. J. Teat and M. Hamichi, *J. Synchrotron Radiat.*, 1997, **4**, 279–286.
- SMART, Bruker AXS Inc., Madison, WI, USA, 1998.
- SAINT, Bruker AXS Inc., Madison, WI, USA, 2000.
- G. M. Sheldrick, *SHELXTL*, Bruker AXS Inc., Madison, WI, USA, 2000.

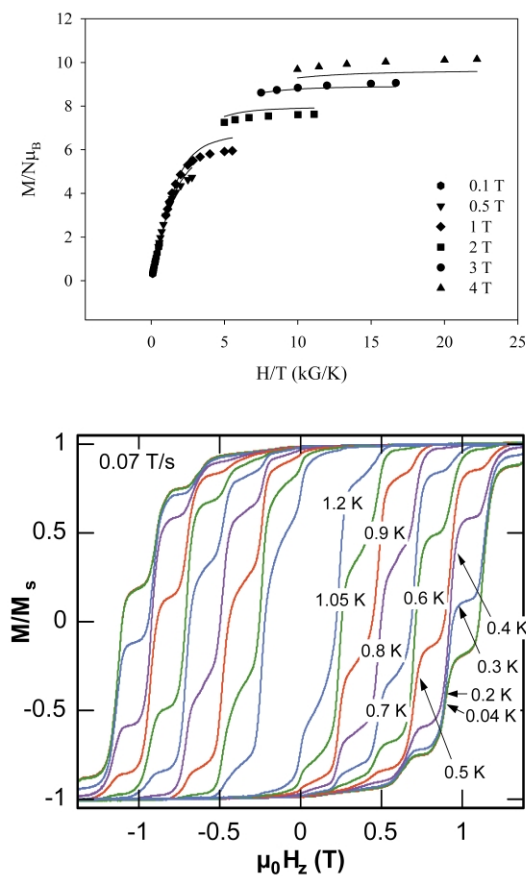


Fig. 2 Plot of reduced magnetization vs. H/T for **2** (top). The solid lines are fits of the data to an $S = 6$ state with $D = -0.36 \text{ K}$ and $g = 1.81$. Magnetization (M) of **1** (bottom) plotted as maximum value M_s vs. applied magnetic field ($\mu_0 H$).